Unified pictures of Q-balls and Q-tubes

Takashi Tamaki*

Department of Physics, General Education, College of Engineering, Nihon University, Tokusada, Tamura, Koriyama, Fukushima 963-8642, Japan

Nobuyuki Sakai†

Department of Education, Yamagata University, Yamagata 990-8560, Japan

(Received 22 August 2012; published 7 November 2012)

While Q-balls have been investigated intensively for many years, another type of nontopological solution, Q-tubes, have not been understood very well. In this paper we make a comparative study of Q-balls and Q-tubes. First, we investigate their equilibrium solutions for four types of potentials. We find, for example, that in some models the charge-energy relation is similar between Q-balls and Q-tubes while in other models the relation is quite different between them. To understand what determines the charge-energy relation, which is a key of stability of the equilibrium solutions, we establish an analytical method to obtain the two limit values of the energy and the charge. Our prescription indicates how the existent domain of solutions and their stability depend on their shape as well as potentials, which would also be useful for a future study of Q-objects in higher-dimensional spacetime.

DOI: 10.1103/PhysRevD.86.105011 PACS numbers: 03.75.Lm, 11.27.+d

I. INTRODUCTION

Among nontopological solitons, Q-balls have attracted much attention because they can exist in all supersymmetric extensions of the Standard Model [1]. Specifically, they can be produced efficiently in the Affleck-Dine (AD) mechanism [2] and could be responsible for baryon asymmetry [3] and dark matter [4]. Q-balls can also influence the fate of neutron stars [5]. Based on these motivations, the stability of Q-balls has been intensively studied [6–9].

In spite of these concerns about Q-balls, other equilibrium solutions have not been studied so much, while topological defects have several types according to the symmetry. For example, observational consequences by cosmic strings, such as gravitational lenses and the gravitational wave, have been argued for years [10].

From this point of view, other types of nontopological solutions may play an important role in the Universe. Recently, two types of nontopological solutions were discussed: Q-tubes and Q-crust, which mean tube-shaped (or stringlike) and crust-shaped solutions, respectively [11]. As for Q-tubes, some numerical studies manifested signs of their appearance. First, it has been reported that a filament structure appears just before Q-ball formation in the numerical simulations and can be the source for gravitational waves [12]. Second, according to the simulations of the collision of two Q-balls, two apparent rings are formed [13]. We conjecture that the filament structure and the rings are Q-tubes.

In Ref. [11], numerical solutions were investigated for the potential,

$$V_3(\phi) := \frac{m^2}{2}\phi^2 - \mu\phi^3 + \lambda\phi^4 \quad \text{with} \quad m^2, \mu, \lambda > 0, \tag{1}$$

which we call the V_3 model. In the case of Q-balls [6–8], however, the charge-energy relation, which is a key of stability of the equilibrium solutions, is quite dependent on potentials $V(\phi)$. Therefore, our first concern is how Q-tube solutions depend on potentials.

Our second concern is how different Q-tubes and Q-balls are in the charge-energy relation. This shape dependence is closely related to the dimension dependence because a cylindrical Q-tube in 3 + 1 spacetime is equivalent to a "Q-ball" in 2 + 1 spacetime if we ignore gravity. If this dimension dependence becomes manifest, it would be useful for investigating other Q-objects or those in higher-dimensional spacetime [14].

For these reasons, in this paper we make a comparative study of Q-balls and Q-tubes. This paper is organized as follows. In Sec. II, we explain briefly what Q-balls and Q-tubes are. In Sec. III, we investigate their equilibrium solutions numerically for four types of potentials. In Sec. IV, we evaluate analytically the limit values of the energy and the charge. In Sec. V, we make our concluding remarks.

II. EQUILIBRIUM SOLUTIONS

Consider an SO(2)-symmetric scalar field $\boldsymbol{\phi} = (\phi_1, \phi_2)$, whose action is given by

$$\mathcal{S} = \int d^4x\left[-\frac{1}{2}\eta^{\mu\nu}\partial_\mu\boldsymbol{\phi}\cdot\partial_\nu\boldsymbol{\phi} - V(\phi)\right], \qquad \phi \equiv \sqrt{\boldsymbol{\phi}\cdot\boldsymbol{\phi}}. \tag{2}$$

*tamaki@ge.ce.nihon-u.ac.jp
†nsakai@e.yamagata-u.ac.jp

A. *Q*-balls

For a Q-ball, we assume spherical symmetry and homogeneous phase rotation,

$$\boldsymbol{\phi} = \phi(r)(\cos\omega t, \sin\omega t). \tag{3}$$

One has a field equation,

$$\frac{d^2\phi}{dr^2} + \frac{2}{r}\frac{d\phi}{dr} + \omega^2\phi = \frac{dV}{d\phi}. \tag{4}$$

This is equivalent to the field equation for a single static scalar field with an effective potential

$$V_\omega = V - \frac{1}{2}\omega^2\phi^2. \tag{5}$$

Equilibrium solutions $\phi(r)$ with a boundary condition

$$\frac{d\phi}{dr}(r=0) = 0, \qquad \phi(r\to\infty) = 0, \tag{6}$$

exist if $\min(V_\omega) < V_\omega(0)$ and $d^2V_\omega/d\phi^2(0) > 0$ [15]. This condition is rewritten as

$$\min\left[\frac{2V}{\phi^2}\right] < \omega^2 < m^2 \equiv \frac{d^2V}{d\phi^2}(0), \tag{7}$$

where we have put $V(0) = 0$ without loss of generality.

For a Q-ball solution, we can define the energy and the charge, respectively, as

$$E = 4\pi\int_0^\infty r^2 dr\left\{\frac{1}{2}\omega^2\phi^2 + \frac{1}{2}\left(\frac{d\phi}{dr}\right)^2 + V\right\},$$
$$Q = 4\pi\omega\int_0^\infty r^2\phi^2 dr. \tag{8}$$

The Q-E relation is a key to understand the stability of equilibrium solutions in terms of catastrophe theory [8].

B. *Q*-tubes

For a Q-tube, we suppose a stringlike configuration,

$$\boldsymbol{\phi} = \phi(R)(\cos(n\varphi + \omega t), \sin(n\varphi + \omega t)), \tag{9}$$

where n is a non-negative integer and (R, φ, z) is the cylindrical coordinate system. The field equation becomes

$$\frac{d^2\phi}{dR^2} + \frac{1}{R}\frac{d\phi}{dR} - \frac{n^2\phi}{R^2} + \omega^2\phi = \frac{dV}{d\phi}. \tag{10}$$

In the case of $n = 0$, the field equation is the same as (4) except for a numerical coefficient. Therefore, Q-ball-like solutions of $\phi(R)$ exist if the condition (7) is satisfied.

In the case of $n \geq 1$, there is no regular solution which satisfies $\phi(0) \neq 0$. However, if we adopt a different boundary condition,

$$\phi(R=0) = \phi(R\to\infty) = 0, \tag{11}$$

there is a new type of regular solution. We introduce an auxiliary variable ψ which is defined by $\phi(R) = R^n\psi(R)$. Then, Eq. (10) becomes

$$\frac{d^2\psi}{dR^2} + \frac{2n+1}{R}\frac{d\psi}{dR} + \omega^2\psi = R^{-n}\frac{dV}{d\phi}\bigg|_{\phi=R^n\psi}. \tag{12}$$

If we choose $\psi(0)$ appropriately, we obtain a solution $\psi(R)$ which is expressed in the Maclaurin series without odd powers in the neighborhood of $R = 0$. In terms of the original variable $\phi(R)$, the nth differential coefficient $\phi^{(n)}(0) = \psi(0)$ should be determined by the shooting method, while any lower derivative vanishes at $R = 0$.

In the same way as for Q-balls [15], the existence of Q-tube solutions can be interpreted as follows. If one regards the radius R as "time" and the scalar amplitude $\phi(R)$ as "the position of a particle," one can understand $n = 0$ solutions in the words of Newtonian mechanics, as shown in Fig. 1(a). Equation (10) describes a one-dimensional motion of a particle under the conserved force due to the potential $-V_\omega(\phi)$ and the "time"-dependent friction $-(1/R)d\phi/dR$. If one chooses the "initial position" $\phi(0)$ appropriately, the static particle begins to roll

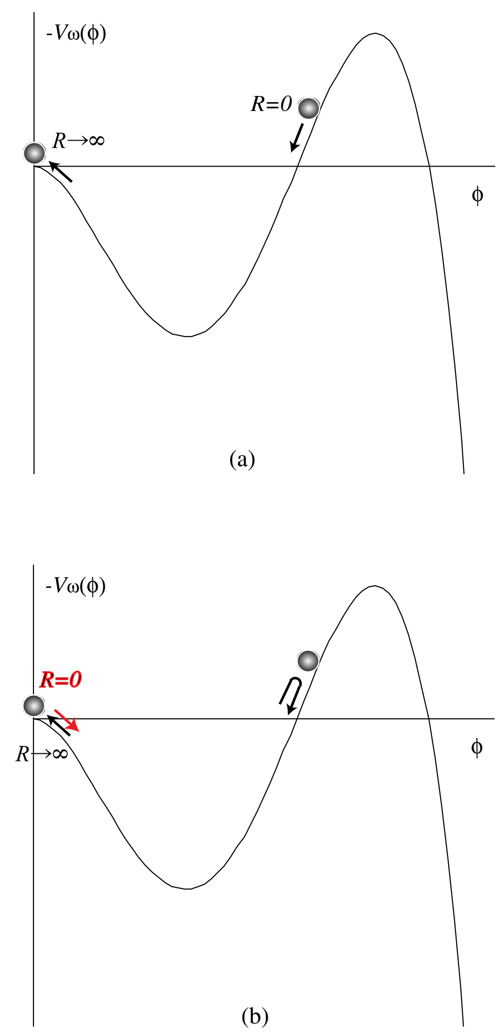

FIG. 1 (color online). Interpretation of (a) Q-balls and $n = 0$ solutions in Q-tubes and (b) $n \geq 1$ solutions in Q-tubes by analogy with a particle motion in Newtonian mechanics.

TABLE I. Two types of Q-balls/Q-tubes solutions and two limits of ω^2.

	Lower limit of ω^2	Upper limit of ω^2
Type I: $\min[V]=0$	$\min[2V/\phi^2]$ (thin)	m^2 (thick)
Type II: $\min[V]<0$	0	m^2 (thick)

down the potential slope, climbs up, and approaches the origin over infinite time.

Similarly, we can also understand the $n \geq 1$ solutions as shown in Fig. 1(b). In this case, there are two nonconserved forces, the friction $-(1/R)d\phi/dR$ and the repulsive force $n^2\phi^2/R^2$. If $n=1$, by choosing the "initial velocity" $d\phi/dR(0)$ appropriately, the particle goes down and up the slope, and at some point, $\phi=\phi_{\max}$, it turns back and approaches the origin over infinite time. If $n \geq 2$, $d\phi/dR(0)$ vanishes; instead, the nth derivative $\phi^{(n)}(0)$ gently pushes the particle at $\phi=0$. Therefore, with the appropriate choice of $\phi^{(n)}(0)$, the particle moves along a similar trajectory to that of $n=1$. This argument also indicates that the existence condition of $n \geq 1$ solutions is the same as that of $n=0$ solutions, (7). Solutions with the same behavior as the $n=1$ solutions were obtained by Kim *et al.* [16], who studied the SO(3)-symmetric scalar field without Q-charge.

Because our Q-tube solutions are infinitely long, the energy and the charge (8) diverge. We therefore define the energy and the charge per unit length, pectively, as

$$e = 2\pi\int_0^\infty RdR\left\{\frac{1}{2}\omega^2\phi^2 + \frac{1}{2}\left(\frac{d\phi}{dR}\right)^2 + \frac{n^2\phi^2}{2R^2} + V\right\},\qquad q = 2\pi\omega\int_0^\infty R\phi^2 dR. \tag{13}$$

C. Two types and two limits

The existence condition (7) indicates that both Q-balls and Q-tubes are classified into two types of solutions according to the sign of $\min[V(\phi)]$.

Type I: $\min[V(\phi)] = V(0) = 0$. In this case, $\min[2V/\phi^2]$ is also positive and the lower limit of ω. The two limits $\omega^2 \to \min[2V/\phi^2]$ and $\omega^2 \to m^2$ correspond to the thin-wall limit and the thick-wall limit, respectively.

Type II: $\min[V(\phi)] < 0$. In this case, $\min[2V/\phi^2]$ is negative. Because $\omega^2 > 0$, there is no thin-wall limit, $\omega^2 \to \min[2V/\phi^2]$. The thick-wall limit, $\omega^2 \to m^2$, still exists.

The two limits of ω^2 for the two types of solutions are summarized in Table I.

III. SOLUTIONS IN VARIOUS POTENTIALS

Here we investigate equilibrium solutions of Q-balls and Q-tubes for four types of potentials.

A. V_3 model

First, we summarize the previous results in the V_3 model (1) [11]. We rescale the quantities as

$$\tilde\phi \equiv \frac{\lambda}{\mu}\phi, \quad \tilde m \equiv \frac{\sqrt{\lambda}}{\mu}m, \quad \tilde\omega \equiv \frac{\sqrt{\lambda}}{\mu}\omega,$$
$$\tilde r \equiv \frac{\mu}{\sqrt{\lambda}}r, \quad \tilde E \equiv \frac{\lambda^{3/2}}{\mu}E, \quad \tilde Q \equiv \lambda Q, \tag{14}$$
$$\tilde R \equiv \frac{\mu}{\sqrt{\lambda}}R, \quad \tilde e \equiv \frac{\lambda^2}{\mu^2}e, \quad \tilde q \equiv \frac{\lambda^{3/2}}{\mu}q,$$

and define a parameter,

$$\epsilon^2 \equiv \tilde m^2 - \tilde\omega^2. \tag{15}$$

Then, the existing condition (7) for the two types becomes

$$0 < \epsilon^2 < \frac{1}{2} \quad \text{for } \tilde m^2 > \frac{1}{2}\text{(type I)},\qquad 0 < \epsilon^2 < \tilde m^2 \quad \text{for } \tilde m^2 < \frac{1}{2}\text{(type II)}. \tag{16}$$

The limits $\epsilon^2 \to 1/2$ and $\epsilon^2 \to 0$ correspond to the thin-wall limit and the thick-wall limit, respectively. As we discussed in the last section, however, in type II solutions there is no thin-wall limit, and the upper limit of ϵ^2 is $\tilde m^2$ instead of $1/2$.

Figure 2 shows examples of the field configurations of Q-tubes. We fix $\tilde m^2 = 0.6$ (type I) and choose $\epsilon^2 = 0.01$ (thick-wall) in (a) and $\epsilon^2 = 0.48$ (thin-wall) in (b). In each diagram we show the three solutions $n = 0, 1,$ and 2, which indicates that the maximum amplitude of the scalar field $\tilde\phi_{\max}$ for $n=0$ is largest among them. We can understand it by analogy with the Newtonian mechanics in Fig. 1. For $n \geq 1$, the particle must make a round-trip while it goes one way for $n=0$. Nevertheless, $\tilde\phi_{\max}$ in all cases is qualitatively unchanged, which means that the conservation law of energy approximately holds in words of the Newtonian mechanics. Of course, the behavior of a Q-ball is similar to that of a Q-tube for $n=0$. These properties are independent of potentials, which is important in understanding Q-balls and Q-tubes in a unified way as we shall see in Sec. IV.

We show the charge-energy-ϵ relations for type I ($\tilde m^2 = 0.6$): Q-balls in Fig. 3 and Q-tubes in Fig. 4. As for Q-tubes, we show results for $n = 0$, 1, and 2. The similarity between Q-balls and Q-tubes is quite remarkable. In the thin-wall limit ($\epsilon^2 \to 1/2$), we confirm that $\tilde Q$, $\tilde E$, $\tilde q$, and $\tilde e$ diverge. In the thick-wall limit ($\epsilon^2 \to 0$), on the other hand, these quantities approach zero.

We also show the same relations for type II ($\tilde m^2 = 0.3$): Q-balls in Fig. 5 and Q-tubes in Fig. 6. The crucial difference from type I is that $\tilde Q$ and $\tilde q$ approach zero in the upper limit $\epsilon^2 \to \tilde m^2$ while $\tilde E$ and $\tilde e$ have nonzero finite values corresponding to the points C. As a result, $\tilde Q$, $\tilde E$, $\tilde q$, and $\tilde e$

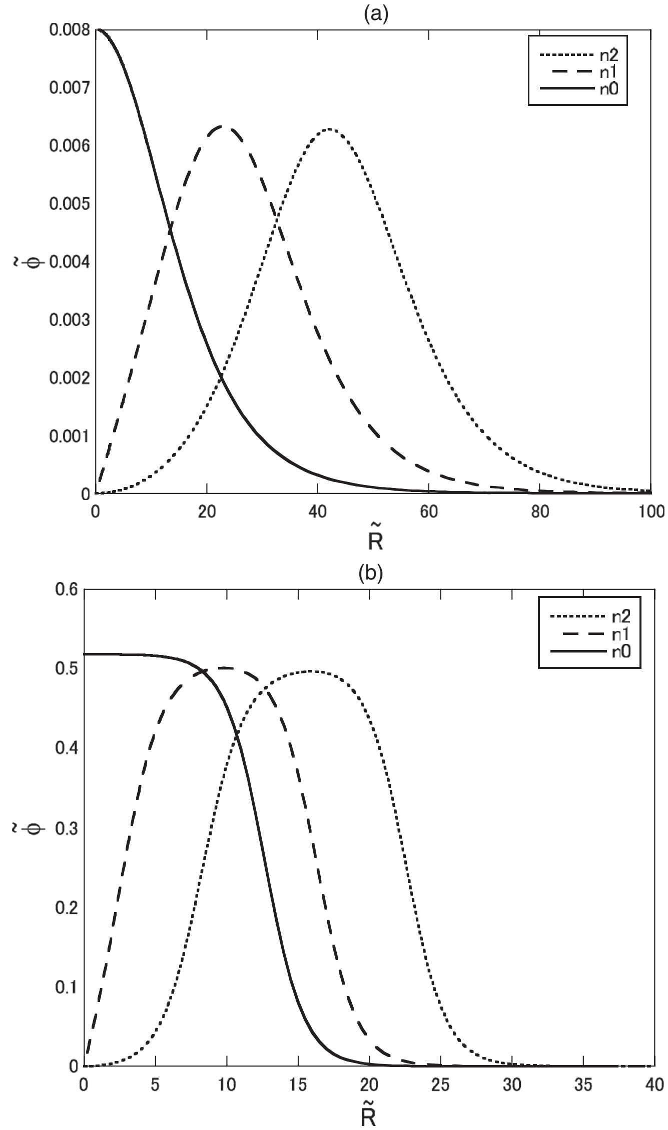

FIG. 2. The field configurations of the scalar field for Q-tubes in the V_3 model with $\tilde{m}^2 = 0.6$ (type I): (a) $\epsilon^2 = 0.01$ (thick-wall) and $\epsilon^2 = 0.48$ (thin-wall).

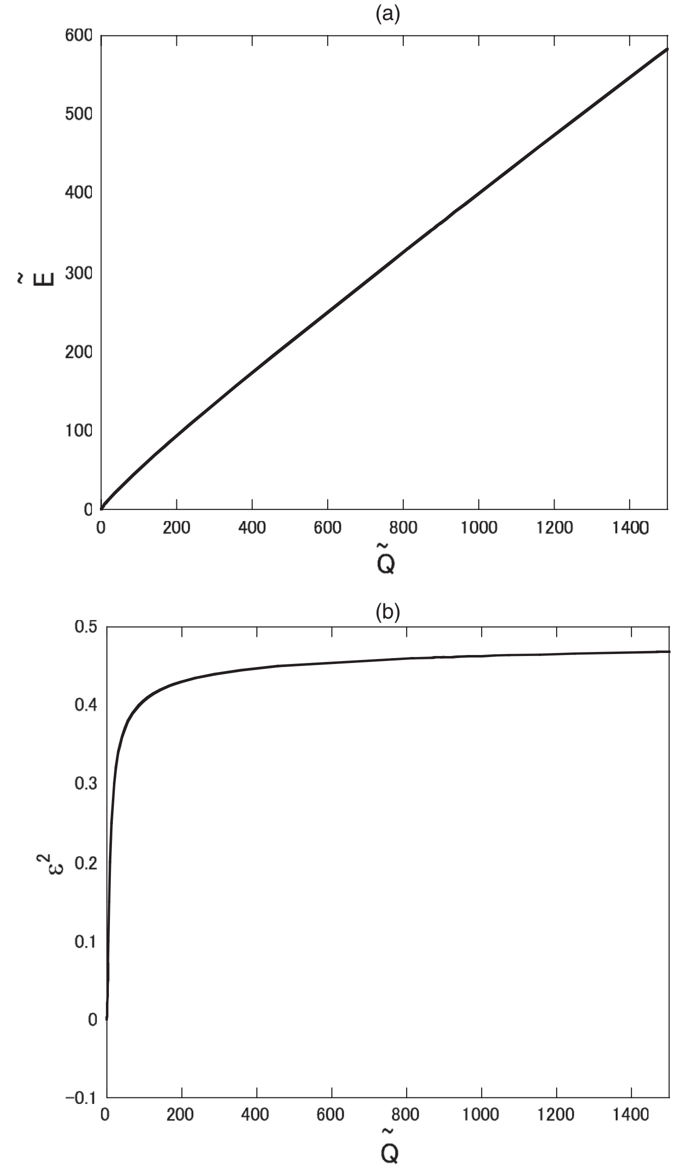

FIG. 3. (a) $\tilde{Q}$-$\tilde{E}$ and (b) $\tilde{Q}$-ϵ^2 relations for type I Q-balls in the V_3 model: $\tilde{m}^2 = 0.6$.

have maximum values for the intermediate value of ϵ^2 corresponding to the points B where cusp structures appear in Figs. 5 and 6(a). The stability of Q-balls and Q-tubes can be understood using catastrophe theory [8,17]. The cusp structures in $\tilde{Q}$-$\tilde{E}$ ($\tilde{q}$-$\tilde{e}$) diagrams mean the stability change in catastrophe theory. The solutions from point A to B are stable while B to C are unstable. The extreme values of the energy and the charge of Q-balls and Q-tubes in the V_3 model are summarized in Table II.

B. The V_4 model

Second, we consider another simple potential,

$$V_4(\phi) := \frac{m^2}{2}\phi^2 - \lambda\phi^4 + \frac{\phi^6}{M^2} \quad \text{with} \quad m^2, \lambda, M^2 > 0, \qquad (17)$$

which we call the V_4 model. We rescale the quantities as

$$\tilde{\phi} \equiv \frac{\phi}{\sqrt{\lambda}M}, \qquad \tilde{m} \equiv \frac{m}{\lambda M}, \qquad \tilde{\omega} \equiv \frac{\omega}{\lambda M},$$
$$\tilde{r} \equiv \lambda M r, \qquad \tilde{E} \equiv \frac{E}{M}, \qquad \tilde{Q} \equiv \lambda Q, \qquad (18)$$
$$\tilde{R} \equiv \lambda M R, \qquad \tilde{e} \equiv \frac{e}{\lambda M^2}, \qquad \tilde{q} \equiv \frac{q}{M},$$

and again define a parameter ϵ by (15).

Then the existing condition is identical to (16) in the V_3 case. We show the charge-energy-ϵ relations in Figs. 7–10: type I Q-balls in Fig. 7, type I Q-tubes in Fig. 8, type II Q-balls in Fig. 9, and type II Q-tubes in Fig. 10. Contrary to the case of the V_3 model, a qualitative difference between Q-tubes and Q-balls appears. The extreme values of the

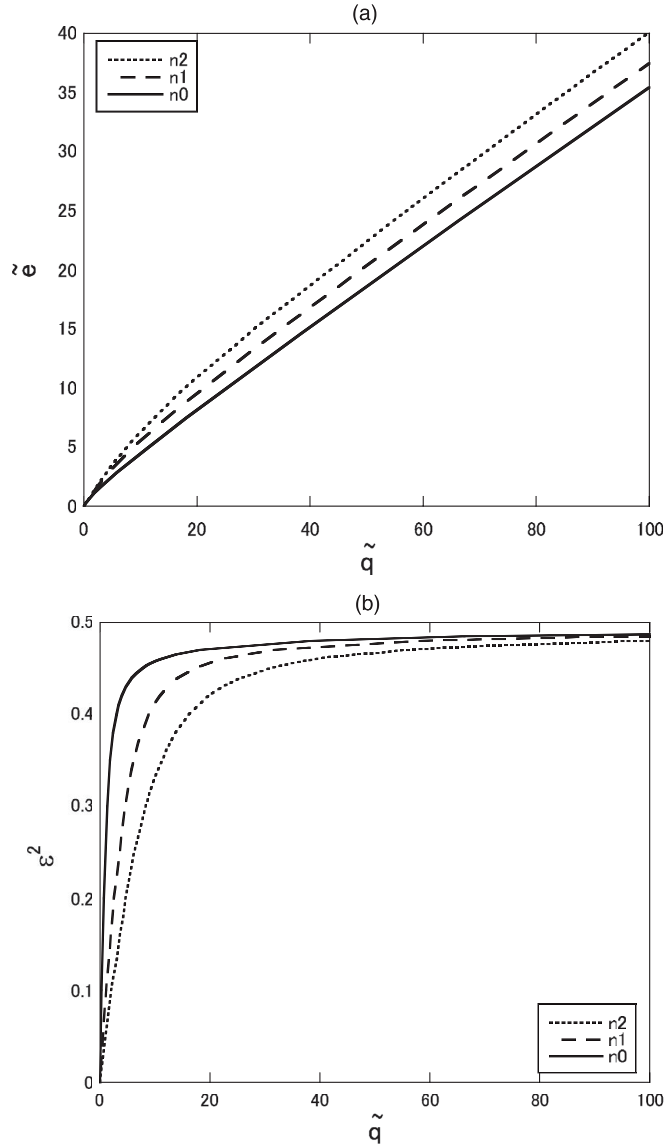

FIG. 4. (a) $\tilde{q}$-$\tilde{e}$ and (b) $\tilde{q}$-ϵ^2 relations for type I Q-tubes in the V_3 model: $\tilde{m}^2 = 0.6$.

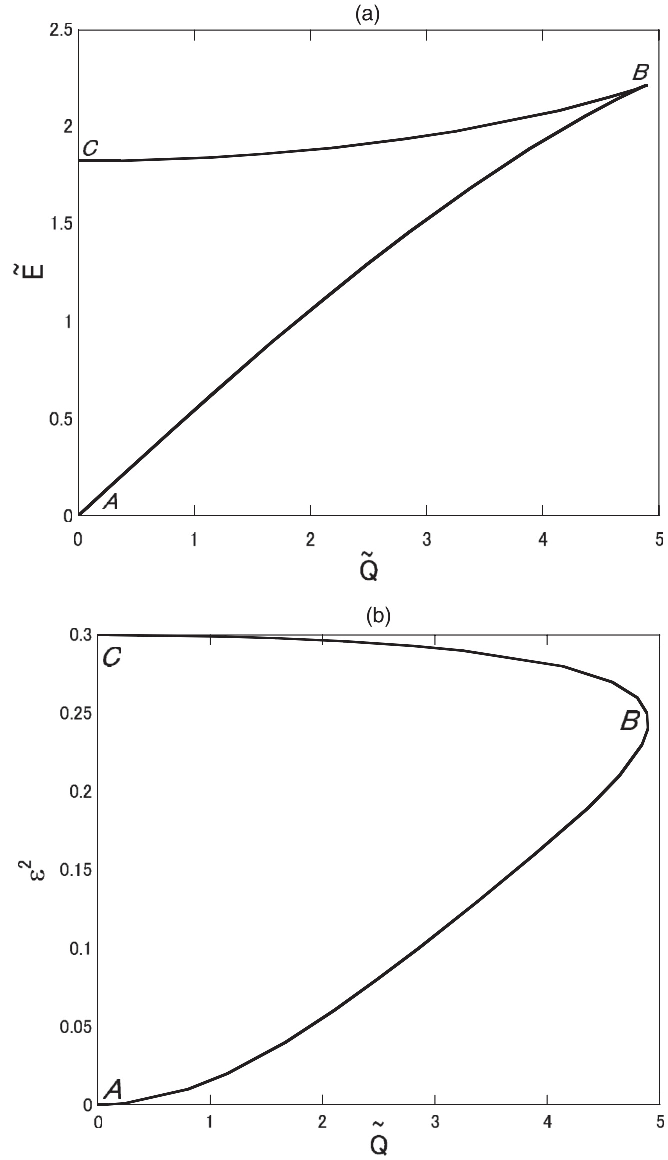

FIG. 5. (a) $\tilde{Q}$-$\tilde{E}$ and (b) $\tilde{Q}$-ϵ^2 relations for type I Q-balls in the V_3 model: $\tilde{m}^2 = 0.3$.

energy and the charge of Q-balls and Q-tubes in the V_4 model are summarized in Table III.

The structures of the solution series of type II Q-balls and Q-tubes are not simple. In the case of Q-balls, there are two cusps in the Q-E diagram, B and C. Only the solutions between these two points represent stable solutions. In the case of Q-tubes, a cusp appears for $n = 0$, while no cusp appears for $n \geq 1$.

C. AD gravity-mediation type

From the theoretical point of view, it is important to investigate Q-tubes as well as Q-balls in the AD mechanism. There are two types of potentials: gravity-mediation type and gauge-mediation type. Here we consider the former type,

$$V_{\rm grav}(\phi) := \frac{m_{\rm grav}^2}{2}\phi^2\left[1 + K\ln\left(\frac{\phi}{M}\right)^2\right] \quad \text{with} \quad m_{\rm grav}^2,\ M > 0. \tag{19}$$

We rescale the quantities as

$$\tilde{\phi} \equiv \frac{\phi}{M}, \quad \tilde{\omega} \equiv \frac{\omega}{m_{\rm grav}}, \quad \tilde{r} \equiv m_{\rm grav} r, \quad \tilde{E} \equiv \frac{m_{\rm grav} E}{M^2}, \quad \tilde{Q} \equiv \frac{m_{\rm grav}^2 Q}{M^2}, \quad \tilde{R} \equiv m_{\rm grav} R, \quad \tilde{e} \equiv \frac{e}{M^2}, \quad \tilde{q} \equiv \frac{m_{\rm grav} q}{M^2}, \tag{20}$$

and define a parameter ϵ as

$$\epsilon^2 = 1 - \tilde{\omega}^2. \tag{21}$$

The existing condition (7) becomes

$$K < 0, \qquad \epsilon^2 < 1. \tag{22}$$

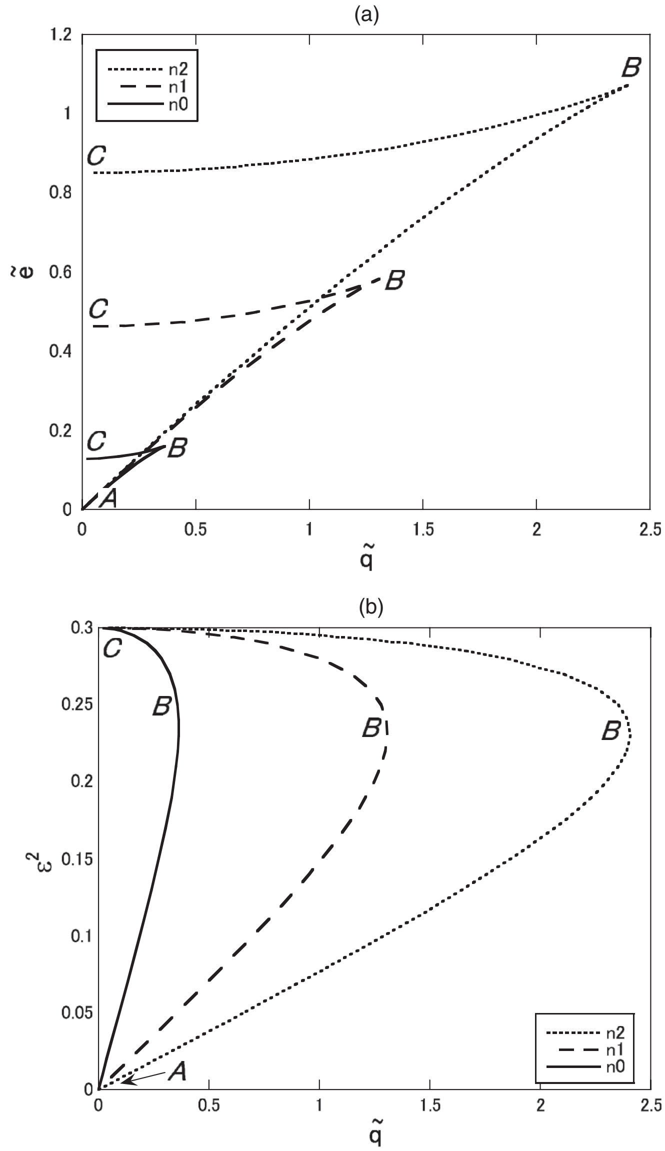

FIG. 6. (a) $\tilde{q}$-$\tilde{e}$ and (b) $\tilde{q}$-ϵ^2 relations for type I Q-tubes in the V_3 model: $\tilde{m}^2 = 0.3$.

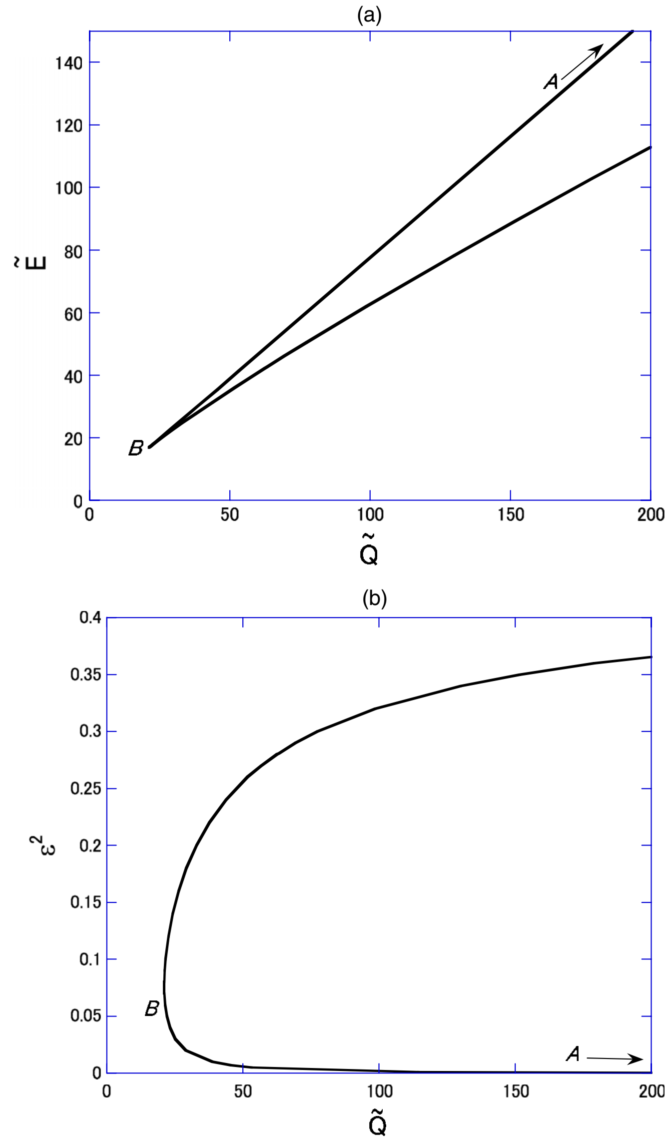

FIG. 7 (color online). (a) $\tilde{Q}$-$\tilde{E}$ and (b) $\tilde{Q}$-ϵ^2 relations for type I Q-balls in the V_4 model: $\tilde{m}^2 = 0.6$.

Thus, ϵ^2 is not bounded below, which is in contrast to the V_3 and V_4 models. Only type II solutions exist in this model unless we introduce additional terms in the potential. We show the charge-energy-ϵ relations: Q-balls in Fig. 11 and Q-tubes in Fig. 12. The extreme values of the energy and the charge of Q-balls and Q-tubes in the gravity-mediation type are summarized in Table IV. There is no qualitative difference in the charge-energy relation between Q-balls and Q-tubes. These properties are common to type II solutions in the V_3 model.

TABLE II. Extreme values of the energy and the charge of Q-balls and Q-tubes in the V_3 model.

	$\epsilon^2 \to \min[1/2, \tilde{m}^2]$	$\epsilon^2 \to 0$ (thick)
Type I: $\tilde{m}^2 > 1/2$	$\tilde{E}, \tilde{Q}, \tilde{e}, \tilde{q} \to \infty$	$\tilde{E}, \tilde{Q}, \tilde{e}, \tilde{q} \to 0$
Type II: $\tilde{m}^2 < 1/2$	$\tilde{E}, \tilde{e} \to$ nonzero finite $\tilde{Q}, \tilde{q} \to 0$	$\tilde{E}, \tilde{Q}, \tilde{e}, \tilde{q} \to 0$

D. AD gauge-mediation type

Finally, we consider the gauge-mediation type in the AD mechanism,

$$V_{\rm gauge}(\phi) := m_{\rm gauge}^4 \ln\left(1 + \frac{\phi^2}{m_{\rm gauge}^2}\right) \quad \text{with} \quad m_{\rm gauge}^2 > 0. \tag{23}$$

We rescale the quantities as

$$\tilde{\phi} \equiv \frac{\phi}{m_{\rm gauge}}, \quad \tilde{\omega} \equiv \frac{\omega}{m_{\rm gauge}}, \quad \tilde{r} \equiv m_{\rm gauge} r, \quad \tilde{E} \equiv \frac{E}{m_{\rm gauge}},$$
$$\tilde{Q} \equiv Q, \quad \tilde{R} \equiv m_{\rm gauge} R, \quad \tilde{e} \equiv \frac{e}{m_{\rm gauge}^2}, \quad \tilde{q} \equiv \frac{q}{m_{\rm gauge}}, \tag{24}$$

and define a parameter ϵ as

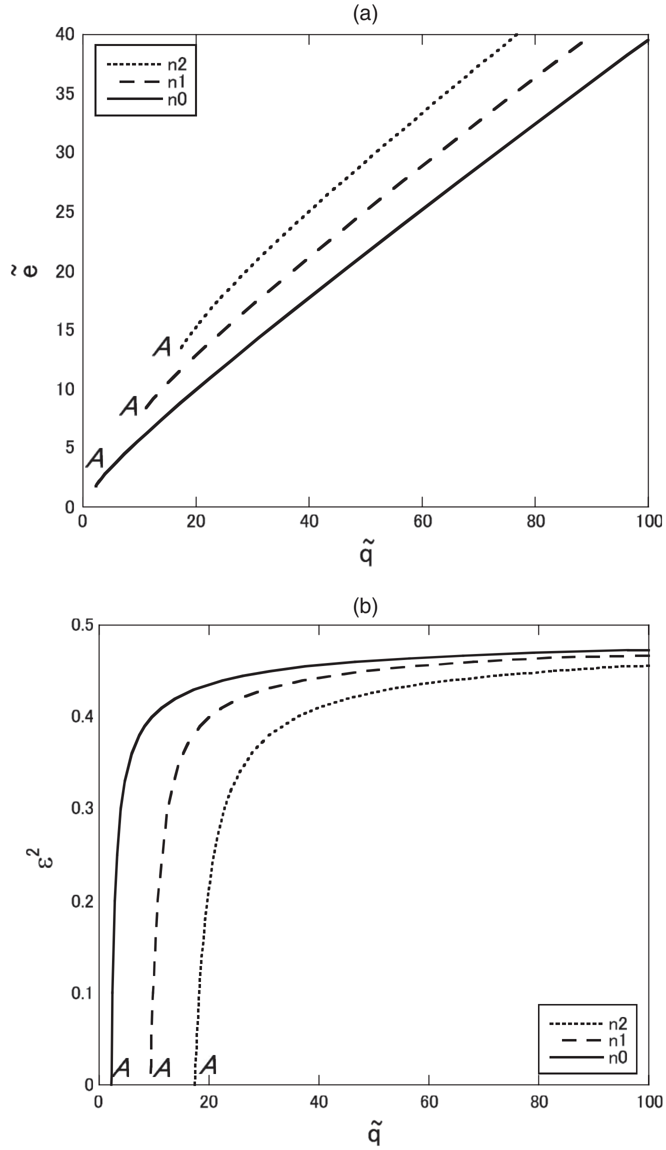

FIG. 8. (a) $\tilde{q}$-$\tilde{e}$ and (b) $\tilde{q}$-ϵ^2 relations for type I Q-tubes in the V_4 model: $\tilde{m}^2 = 0.6$.

$$\epsilon^2 = 2 - \tilde{\omega}^2. \tag{25}$$

Then the existing condition (7) becomes

$$0 < \epsilon^2 < 2. \tag{26}$$

Only type I solutions exist in this model. We show the charge-energy-ϵ relation: Q-balls in Fig. 13 and Q-tubes in Fig. 14. The extreme values of the energy and the charge of Q-balls and Q-tubes in the gravity-mediation type are summarized in Table V. These properties are common to the type I solutions in the V_4 model.

IV. UNIFIED PICTURE OF Q-BALLS AND Q-TUBES

Our numerical results in the last section indicate that the charge-energy relation of equilibrium solutions depends a great deal on functional forms of the potential $V(\phi)$. In this section we discuss what determines the extreme values of the energy and the charge by analytical methods. As we explained in Sec. II, we can understand Q-balls and Q-tubes in words of a particle motion in Newtonian mechanics. In Fig. 1, if we ignore "nonconserved force," the maximum of ϕ, $\tilde{\phi}_{\max}$ is determined by the nontrivial solution of $V_\omega = 0$. Using this $\tilde{\phi}_{\max}$, we can evaluate the order of magnitude of the energy and the charge, (8) and (13), as

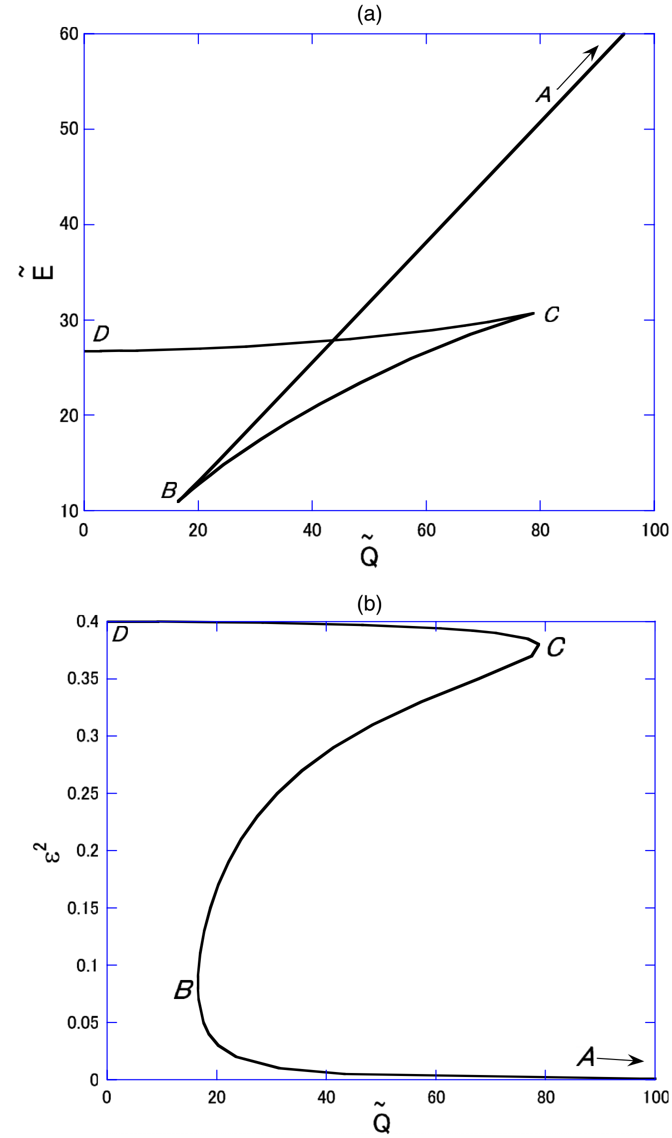

FIG. 9 (color online). (a) $\tilde{Q}$-$\tilde{E}$ and (b) $\tilde{Q}$-ϵ^2 relations for type II Q-balls in the V_4 model: $\tilde{m}^2 = 0.4$.

$$\begin{aligned}
&\tilde{E} \sim \tilde{r}^3_{\max}\left\{\frac{1}{2}\tilde{\omega}^2\tilde{\phi}^2_{\max} + \frac{1}{2}\left(\frac{d\tilde{\phi}}{d\tilde{r}}\right)^2 + \tilde{V}\right\},\\
&\tilde{Q} \sim \tilde{\omega}\tilde{r}^3_{\max}\tilde{\phi}^2_{\max},\\
&\tilde{e} \sim \tilde{R}^2_{\max}\left\{\frac{1}{2}\tilde{\omega}^2\tilde{\phi}^2_{\max} + \frac{1}{2}\left(\frac{d\tilde{\phi}}{d\tilde{R}}\right)^2 + \frac{n^2\tilde{\phi}^2_{\max}}{2\tilde{R}^2_{\max}} + \tilde{V}\right\},\\
&\tilde{q} \sim \tilde{\omega}\tilde{R}^2_{\max}\tilde{\phi}^2_{\max},
\end{aligned} \tag{27}$$

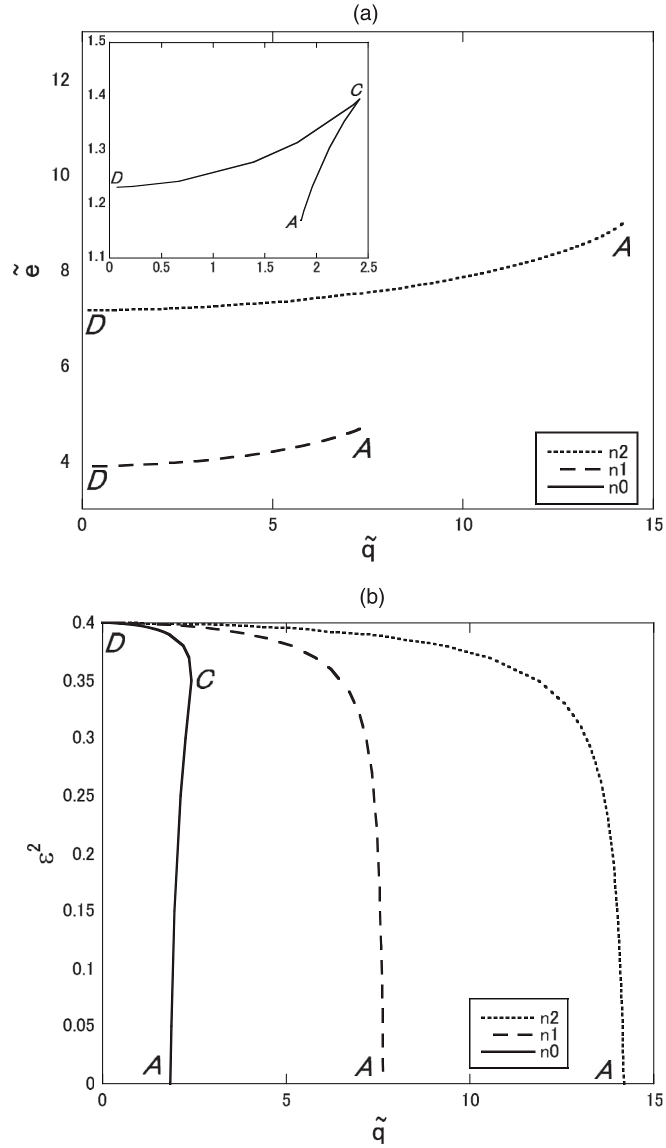

FIG. 10. (a) $\tilde{q}$-$\tilde{e}$ and (b) $\tilde{q}$-ϵ^2 relations for type II Q-tubes in the V_4 model: $\tilde{m}^2 = 0.4$.

where the subscript "max" denotes the values at which $\tilde{\phi} = \tilde{\phi}_{\rm max}$. As for $\tilde{R}_{\rm max}$ for $n = 0$ or $\tilde{r}_{\rm max}$, it is reasonable to take $\tilde{R}$ or $\tilde{r}$ where $\tilde{\phi}$ becomes about $0.5\tilde{\phi}_{\rm max}$.

What we want to discuss is whether $\tilde{E}$, $\tilde{Q}$, $\tilde{e}$, and $\tilde{q}$ approach zero, infinity, or nonzero finite values as ϵ^2 approaches the upper or lower limit. The approximate expression (27) is appropriate for this purpose.

TABLE III. Extreme values of the energy and the charge of Q-balls and Q-tubes in the V_4 model.

	$\epsilon^2 \to \min[1/2, \tilde{m}^2]$	$\epsilon^2 \to 0$ (thick)
Type I: $\tilde{m}^2 > 1/2$	$\tilde{E}$, $\tilde{Q}$, $\tilde{e}$, $\tilde{q} \to \infty$	$\tilde{E}$, $\tilde{Q} \to \infty$
		$\tilde{e}$, $\tilde{q} \to$ nonzero finite
Type II: $\tilde{m}^2 < 1/2$	$\tilde{E}$, $\tilde{e} \to$ nonzero finite	$\tilde{E}$, $\tilde{Q} \to \infty$
	$\tilde{Q}$, $\tilde{q} \to 0$	$\tilde{e}$, $\tilde{q} \to$ nonzero finite

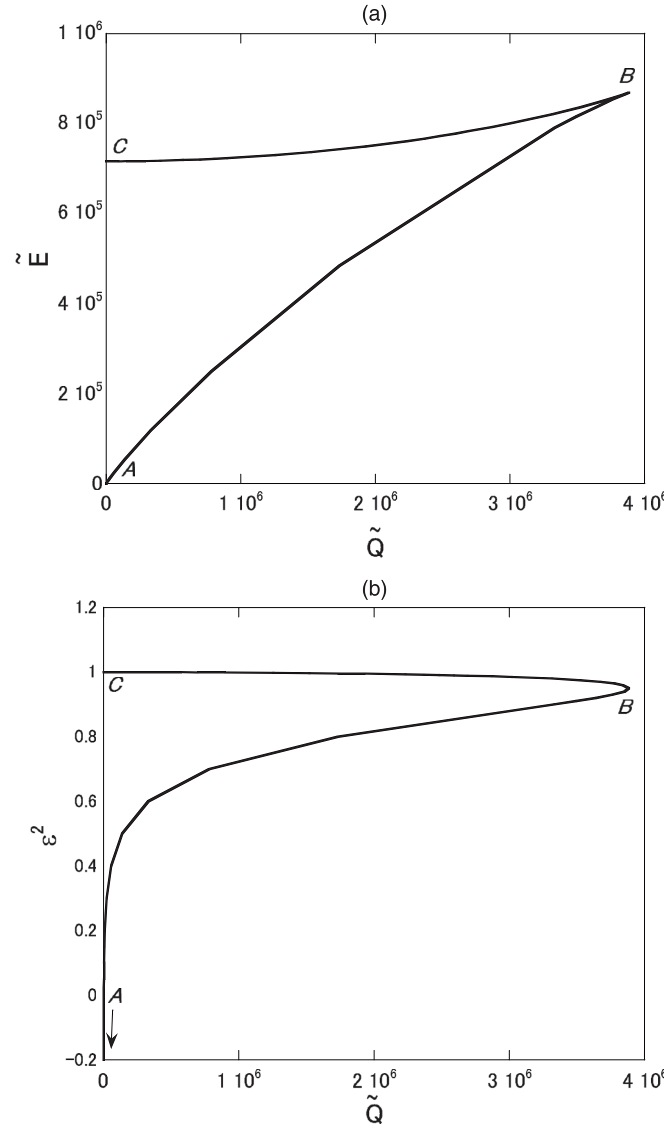

FIG. 11. (a) $\tilde{Q}$-$\tilde{E}$ and (b) $\tilde{Q}$-ϵ^2 relations for $V_{\rm grav}$: $K = -0.1$.

First, we discuss the upper limit of ϵ^2, or equivalently, the lower limit of ω^2. In type I solutions, where $\min[V] = V(0) = 0$, in the limit of $\omega \to \min[2V/\phi^2]$, the minimum of V_ω approaches zero. In this case, in the Newtonian-mechanics picture of Fig. 1, a particle rolls down from the top of the hill over infinite time, i.e., $R_{\rm max}$ diverges. This limit corresponds to the thin-wall limit. From the expression (27), we see that $\tilde{Q}$, $\tilde{E}$, $\tilde{q}$, and $\tilde{e}$ diverge.

On the other hand, in the type II solutions, where $\min[V] < 0$, because $V_\omega < V$, there is no limit of $\min V_\omega \to 0$. Therefore, $\tilde{Q}$, $\tilde{E}$, $\tilde{q}$, and $\tilde{e}$ must have their upper limits.

Next, we investigate the lower limit of ϵ^2, or equivalently, the upper limit of ω^2. This limit corresponds to the thick-wall limit. Except for the $V_{\rm grav}$ model, ϵ satisfies

$$\epsilon^2 = \frac{d^2\tilde{V}_\omega}{d\tilde{\phi}^2}(0), \tag{28}$$

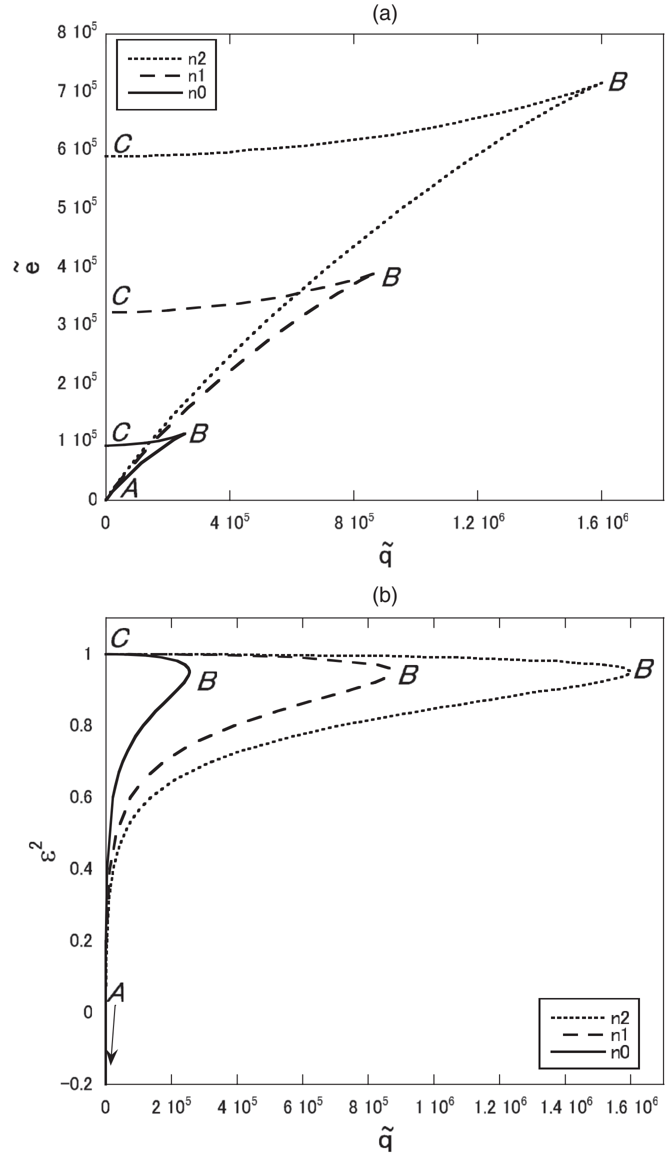

FIG. 12. (a) $\tilde{q}$-$\tilde{e}$ and (b) $\tilde{q}$-ϵ^2 relations for $V_{\rm grav}$: $K = -0.1$.

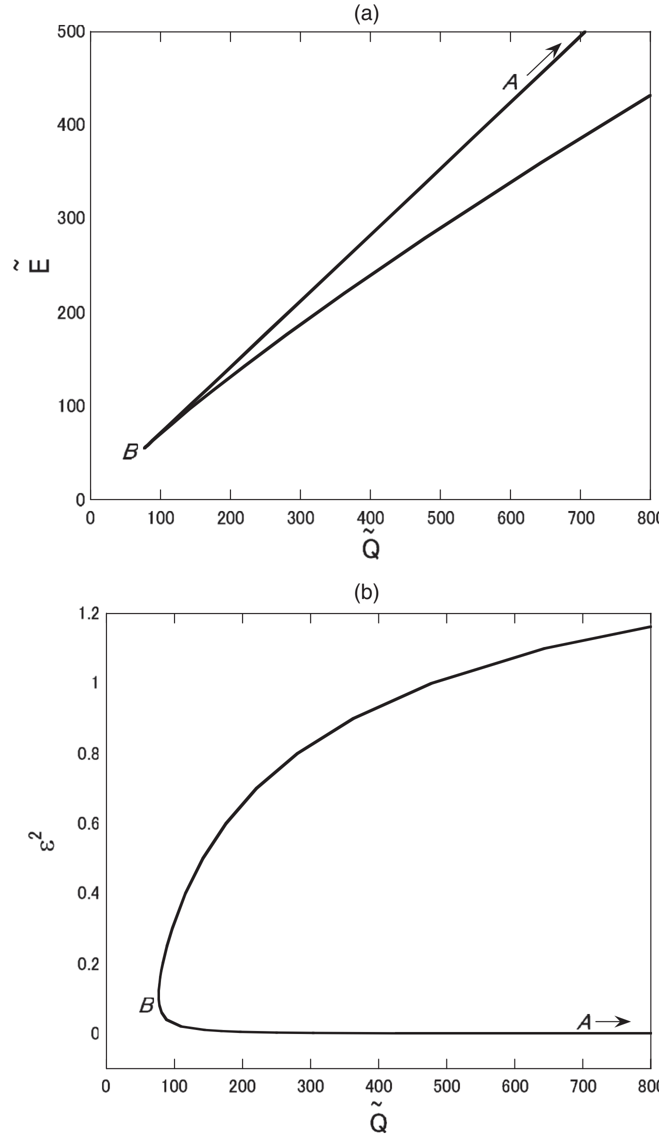

FIG. 13. (a) $\tilde{Q}$-$\tilde{E}$ and (b) $\tilde{Q}$-ϵ^2 relations for $V_{\rm gauge}$.

which means that ϵ is the mass scale of V_ω. If we remember that the Compton wavelength of a particle is inverse of the particle mass, the wall thickness is of order of $1/\epsilon$. Because the radius and the wall thickness are of the same order in the thick-wall limit, except for the $V_{\rm grav}$ model, we obtain

$$\tilde{r}_{\rm max}, \tilde{R}_{\rm max} \sim \frac{1}{\epsilon}. \tag{29}$$

TABLE IV. Extreme values of the energy and the charge of Q-balls and Q-tubes in the AD gravity-mediation type.

	$\epsilon^2 \to 1$	$\epsilon^2 \to -\infty$ (thick)
Type II	$\tilde{E}$, $\tilde{e} \to$ nonzero finite $\tilde{Q}$, $\tilde{q} \to 0$	$\tilde{E}$, $\tilde{Q}$, $\tilde{e}$, $\tilde{q} \to 0$

In the following, from the approximate expressions (27) and (29) we evaluate the limits of the charge and the energy as ϵ approaches the lower limit. Since $\tilde{\phi}$ can be approximated by a constant in this limit, we concentrate on evaluating $\tilde{\phi}_{\rm max}$.

(A) V_3 *case*

The solution of $V_\omega = 0$ is

$$\tilde{\phi}_{\rm max} = \frac{1 - \sqrt{1 - 2\epsilon^2}}{2}. \tag{30}$$

In the lower limit $\epsilon^2 \to 0$, we have $\tilde{\phi}_{\rm max} \simeq \epsilon^2/2$. Therefore, from Eqs. (27)–(29), we find

$$\tilde{Q}, \tilde{E}, \tilde{q}, \tilde{e} \to 0, \tag{31}$$

which agree with the numerical results in Table II.

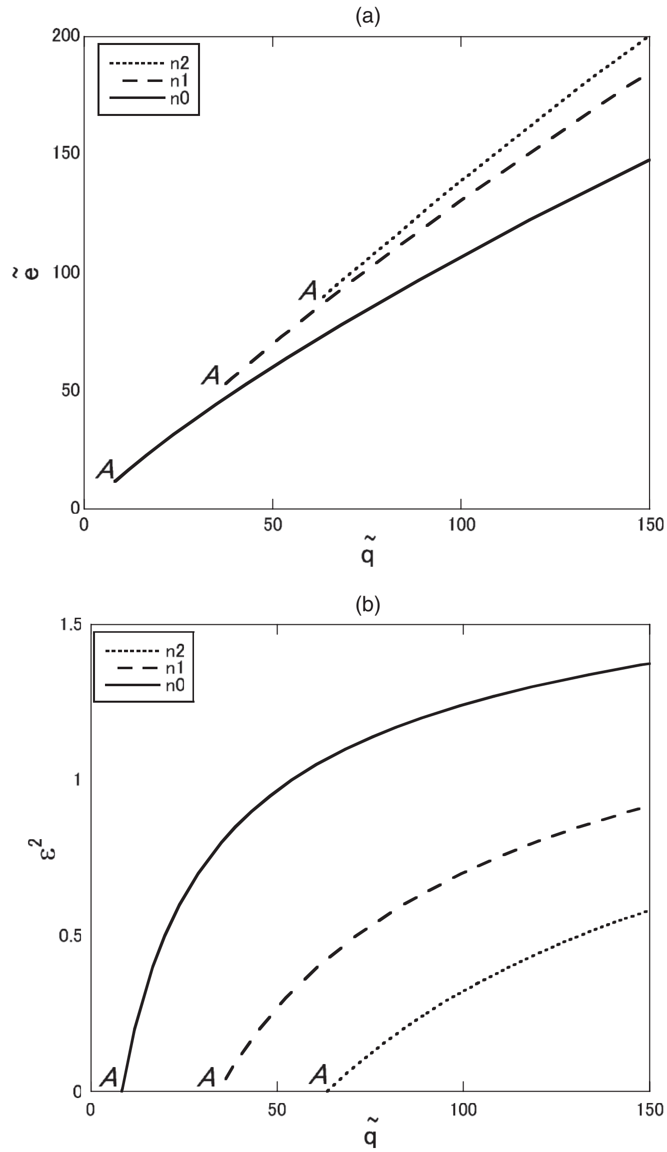

FIG. 14. (a) $\tilde{q}$-$\tilde{e}$ and (b) $\tilde{q}$-ϵ^2 relations for $V_{\rm gauge}$.

(B) V_4 *case*
From $V_\omega = 0$, we obtain

$$\tilde{\phi}^2_{\rm max} = \frac{1 - \sqrt{1 - 2\epsilon^2}}{2}. \tag{32}$$

In the lower limit $\epsilon^2 \to 0$, we have $\tilde{\phi}_{\rm max} \simeq \epsilon$. Substituting this and (29) into (27), we have

$$\tilde{E} \sim \frac{1}{\epsilon^3}\frac{1}{2}\tilde{\omega}^2\epsilon^2 \to \infty, \qquad \tilde{Q} \sim \tilde{\omega}\frac{1}{\epsilon^3}\epsilon^2 \to \infty,$$
$$\tilde{e} \sim \frac{1}{\epsilon^2}\frac{1}{2}\tilde{\omega}^2\epsilon^2 \to {\rm const}, \qquad \tilde{q} \sim \tilde{\omega}\frac{1}{\epsilon^2}\epsilon^2 \to {\rm const}, \tag{33}$$

which agree with the numerical results in Table III. This explains why the results between Q-tubes and Q-balls are different in this model while no qualitative difference appears in the V_3 model.

(C) $V_{\rm grav}$ *case*
The solution of $V_\omega = 0$ is

$$\tilde{\phi}_{\rm max} = e^{-\frac{\epsilon^2}{2K}}. \tag{34}$$

We note that dependence on K is exteremely large. $\tilde{\phi}_{\rm max}$ approaches zero in the lower limit $\epsilon^2 \to -\infty$. Since $R_{\rm max}$ does not diverge,

$$\tilde{Q}, \tilde{E}, \tilde{q}, \tilde{e} \to 0, \tag{35}$$

which agree with the numerical results in Table IV. In a realistic situation, we anticipate that $V_{\rm grav}$ has also the nonrenormalization term $\tilde{V}_{\rm NR} = \beta\tilde{\phi}^n$ where $\beta > 0$ and $n > 2$. This does not change the qualitative behavior in the lower limit. However, in the upper limit, $V_\omega = 0$ has degenerate solutions as in type I models. Therefore, we anticipate that the charge-energy relation for $V_{\rm grav}$ with $\tilde{V}_{\rm NR}$ is similar to that for type I solutions in the V_3 model.

(D) $V_{\rm gauge}$ *case*
We should solve

$$\ln(1 + \tilde{\phi}^2_{\rm max}) = \frac{\tilde{\omega}^2\tilde{\phi}^2_{\rm max}}{2}. \tag{36}$$

In the lower limit $\epsilon^2 \to 0$, if we use the Maclaurin expansion and neglect higher order terms $O(\tilde{\phi}^5_{\rm max})$, we have

$$\tilde{\phi}^2_{\rm max}\epsilon^2 \simeq \tilde{\phi}^4_{\rm max}. \tag{37}$$

Then, we obtain

$$\tilde{\phi}_{\rm max} \simeq \epsilon, \tag{38}$$

as in the V_4 model. Therefore, the limit values are identical to (33), which agree with the numerical results in Table V. We also understand why the results for V_4 with $\tilde{m}^2 > 1/2$ and for $V_{\rm gauge}$ are qualitatively the same [18].

TABLE V. Extreme values of the energy and the charge of Q-balls and Q-tubes in the AD gauge-mediation type.

	$\epsilon^2 \to 2$ (thin)	$\epsilon^2 \to 0$ (thick)
Type I	$\tilde{E}$, $\tilde{Q}$, $\tilde{e}$, $\tilde{q} \to \infty$	$\tilde{E}$, $\tilde{Q} \to \infty$ $\tilde{e}$, $\tilde{q} \to$ nonzero finite

V. SUMMARY AND DISCUSSIONS

We have made a comparative study of Q-balls and Q-tubes. First, we investigated their equilibrium solutions for four types of potentials. The charge-energy relation depends on potential models. We also noted that in some models the charge-energy relation is similar between

Q-balls and Q-tubes while in other models the relation is quite different between them. To understand what determines the charge-energy relation, which is a key of stability of the equilibrium solutions, we established an analytical method to obtain the two limit values of the energy and the charge. Our results indicated how the existent domain of solutions and their stability depends on their shape as well as potentials. This method would also be useful for other Q-objects or those in higher-dimensional spacetime. These are our next subjects.

ACKNOWLEDGMENTS

We would like to thank Kei-ichi Maeda for continuous encouragement. The numerical calculations were carried out on SX8 at YITP in Kyoto University.

---

[1] A. Kusenko, Phys. Lett. B **405**, 108 (1997); Nucl. Phys. B, Proc. Suppl. **62**, 248 (1998).

[2] I. Affleck and M. Dine, Nucl. Phys. **B249**, 361 (1985).

[3] K. Enqvist and J. McDonald, Phys. Lett. B **425**, 309 (1998); Nucl. Phys. **B538**, 321 (1999); S. Kasuya and M. Kawasaki, Phys. Rev. D **62**, 023512 (2000).

[4] A. Kusenko and M. Shaposhnikov, Phys. Lett. B **418**, 46 (1998); K. Enqvist, S. Kasuya, and A. Mazumdar, Phys. Rev. D **66**, 043505 (2002); K. Enqvist and A. Mazumdar, Phys. Rep. **380**, 99 (2003); I. M. Shoemaker and A. Kusenko, Phys. Rev. D **80**, 075021 (2009).

[5] A. Kusenko, M. Shaposhnikov, P. G. Tinyakov, and I. I. Tkachev, Phys. Lett. B **423**, 104 (1998).

[6] A. Kusenko, Phys. Lett. B **404**, 285 (1997); **406**, 26 (1997); T. Multamaki and I. Vilja, Nucl. Phys. **B574**, 130 (2000); M. Axenides, S. Komineas, L. Perivolaropoulos, and M. Floratos, Phys. Rev. D **61**, 085006 (2000); M. I. Tsumagari, E. J. Copeland, and P. M. Saffin, *ibid.* **78**, 065021 (2008).

[7] F. Paccetti Correia and M. G. Schmidt, Eur. Phys. J. C **21**, 181 (2001).

[8] N. Sakai and M. Sasaki, Prog. Theor. Phys. **119**, 929 (2008).

[9] T. Tamaki and N. Sakai, Phys. Rev. D **81**, 124041 (2010); **83**, 044027 (2011); **83**, 084046 (2011); **84**, 044054 (2011).

[10] For a review, see, e.g., A. Vilenkin and E. P. S. Shellard, *Cosmic Strings and Other Topological Defects* (Cambridge University Press, Cambridge, England, 1994).

[11] N. Sakai, H. Ishihara, and K. Nakao, Phys. Rev. D **84**, 105022 (2011).

[12] K. Enqvist, A. Jokinen, T. Multamaki, and I. Vilja, Phys. Rev. D **63**, 083501 (2001); A. Kusenko and A. Mazumdar, Phys. Rev. Lett. **101**, 211301 (2008); A. Kusenko, A. Mazumdar, and T. Multamaki, Phys. Rev. D **79**, 124034 (2009); E. J. Copeland and M. I. Tsumagari, *ibid.* **80**, 025016 (2009); T. Hiramastu, M. Kawasaki, and F. Takahashi, J. Cosmol. Astropart. Phys. 1006 (2010) 008.

[13] R. Battye and P. Sutcliffe, Nucl. Phys. **B590**, 329 (2000); M. I. Tsumagari, http://www.nottingham.ac.uk/~ppzphy7/webpages/people/Mitsuo/welcome.html.

[14] M. I. Tsumagari, E. J. Copeland, and P. M. Saffin, Phys. Rev. D **78**, 065021 (2008).

[15] S. Coleman, Nucl. Phys. **B262**, 263 (1985).

[16] Y. Kim, K. Maeda, and N. Sakai, Nucl. Phys. **B481**, 453 (1996); Y. Kim, S. J. Lee, K. Maeda, and N. Sakai, Phys. Lett. B **452**, 214 (1999).

[17] For a review of catastrophe theory, see, e.g., T. Poston and I. N. Stewart, *Catastrophe Theory and Its Application* (Pitman, New York, 1978).

[18] In Ref. [12], the potential $V(\phi) = \frac{1}{2}m^2\Lambda^2(1 - e^{-\phi^2/\Lambda^2})$ has been used as an approximation of the AD gauge-mediation model. If we use the Maclaurin expansion also in this case, we obtain (38) again (Λ is the SUSY broken scale).